Structure And Electrochemical Performance Of Spinel- Limn2O4

Conference Paper · June 2014

CITATIONS
0

READS
91

7 authors, including:

Teguh Yulius Surya Panca Putra
Badan Tenaga Nuklir Nasional
14 PUBLICATIONS **61** CITATIONS
SEE PROFILE

Evvy Kartini
National Nuclear Energy Agency , Indonesia (Badan Tenaga Nuklir Nasional)
129 PUBLICATIONS **253** CITATIONS
SEE PROFILE

Kamiyama Takashi
High Energy Accelerator Research Organization
250 PUBLICATIONS **3,083** CITATIONS
SEE PROFILE

THE EFFECT OF ANNEALING TEMPERATURE ON MORPHOLOGY, STRUCTURE AND ELECTROCHEMICAL PERFORMANCE OF SPINEL- $LIMN_2O_4$

TEGUH YULIUS SURYA PANCA PUTRA

Center for Science and Technology of Advanced Materials, National Nuclear Energy Agency (BATAN), Kawasan Puspiptek Serpong, Tangerang Selatan 15314, Indonesia

EVVY KARTINI

Center for Science and Technology of Advanced Materials, National Nuclear Energy Agency (BATAN), Kawasan Puspiptek Serpong, Tangerang Selatan 15314, Indonesia

DESWITA

Center for Science and Technology of Advanced Materials, National Nuclear Energy Agency (BATAN), Kawasan Puspiptek Serpong, Tangerang Selatan 15314, Indonesia

MASAO YONEMURA

High Energy Accelerator Research Organization (KEK), 1-1 Oho, Tsukuba, Ibaraki 305-0801, Japan

SHUKI TORII

High Energy Accelerator Research Organization (KEK), 1-1 Oho, Tsukuba, Ibaraki 305-0801, Japan

TORU ISHIGAKI

Frontier Research Center for Applied Atomic Science, Ibaraki University (iFRC), IQBRC, Shirakata 162-1, Tokai Village, Naka-gun, Ibaraki 319-1106, Japan

TAKASHI KAMIYAMA

High Energy Accelerator Research Organization (KEK), 1-1 Oho, Tsukuba, Ibaraki 305-0801, Japan

The development of lithium ion battery technology is very important in its utilization as a new energy sources, for example in electrical vehicle (EV). One of the components that affect the performance of the battery is the cathode, such as spinel $LiMn_2O_4$. In an effort to obtain a good cathode material it is necessary to set the proper synthesis conditions. In this study, spinel $LiMn_2O_4$ powder was synthesized from $LiOH.H_2O$ and MnO_x by mechanical alloying (MA) method followed by heat treatment at 700°C, 800°C and 900°C. The influence of morphology and crystal structure of the spinel $LiMn_2O_4$ as a

Proceedings of the 14th Asian Conference on Solid State Ionics (ACSSI 2014)

ISBN: 978-981-09-1137-9
doi:10.3850/978-981-09-1137-9_153

result of heat treatment on electrochemical performance was investigated. Observation by SEM showed that the higher the annealing temperature, the crystallinity of the powder particles of the spinel $LiMn_2O_4$ increased. Phase and crystal structure analysis by XRD showed that the purity and crystallinity of the spinel $LiMn_2O_4$ increased with annealing temperature, characterized by sharper peaks of the diffraction patterns. Crystal structure analysis by neutron powder diffraction (NPD) showed that $LiMn_2O_4$ synthesized has spinel structure with space group *Fd-3m* and lattice parameter of 8.233316(8) Å, 8.239790(5) Å and 8.244564(4) Å for annealing temperatures of 700°C, 800°C and 900°C. It is also found that the electrochemical performance of $LiMn_2O_4$ cathode in Li-ion battery increased with annealing temperature, shown by capacity of 248.95 $mAhg^{-1}$, 264.29 $mAhg^{-1}$and 277.24 $mAhg^{-1}$. These results show that increasing purity and crystallinity of the cathode material $LiMn_2O_4$ are significantly affect the electrochemical performance of Li-ion battery.

1. Introduction

In an effort to find new energy sources for wide applications, such as in electrical vehicle (EV), the development of Li-ion battery technology is very important. Cathode materials, such as spinel $LiMn_2O_4$, also affect the performance of the Li-ion battery. Spinel $LiMn_2O_4$ has attracted attention, both in terms of its structure and application, in an effort to find a suitable material for cathode in Li-ion battery system. $LiMn_2O_4$ has advantageous such as relatively low toxicity, cheaper, easiness in preparation, better electrochemical performance etc. $LiMn_2O_4$ is also known to have large rechargeable capacity of 120 mAh/g in the 4V region, which is slightly smaller than that of $LiCoO_2$ (150 mAh/g) and $LiNiO_2$ (200 mAh/g) [1-16].

The physical and electrochemical properties of the material are determined by some factors such as particle size, lattice parameter, stoichiometry, average Mn valence, surface morphology and homogeneity [4,12]. In practice, these factors are closely related to the synthesis condition, such as heating temperature, holding time as well as cooling rate. It will affect the cathodic properties of the lithium transition metal oxides. Another factors such as starting material and the content of lithium is also known to determine the properties of $LiMn_2O_4$ [17].

Various methods have been proposed in order to synthesize $LiMn_2O_4$ with best performance such as conventional solid-state reaction [18-21], sol-gel method [22-24], combustion technique [25], molten salt technique [26], melt impregnation technique [27-29], simple soft-chemical technique [30], co-doping anti-electricity ions [31]. Recently, mechanical alloying (MA) has become a popular method and widely used as an alternative to the solid-state reaction. MA is expected to be an easy, effective, low energy expenses and low-cost method, which offer alternative to conventional high temperature synthesis or solution

chemistry, giving a product of spinel with controllable properties. Many works have been done to study the spinel $LiMn_2O_4$ synthesized by MA method [2-11]. Related to structural study, an accurate and precise method supported by sophisticated facility and instrument, i.e. neutron powder diffraction (NPD), is indispensable.

In this paper, the relationship among synthesis condition by MA, the annealing temperature, and the crystal structure of the spinel $LiMn_2O_4$ will be studied by several methods, namely by Scanning Electron Microscope (SEM) and X-Ray Diffraction (XRD). In order to obtain the information of the occupancy of the atoms, it is important to perform high-resolution NPD. The highest capacity of Li-ion batteries using cathode $LiMn_2O_4$ will be determined by electrochemical measurement. It is expected that the optimum composition of the spinel $LiMn_2O_4$ will replace the existing cathode of Li-ion battery.

2. Experimental Method

Spinels $LiMn_2O_4$ were synthesized from mixtures of stoichiometric amount of $LiOH{\cdot}H_2O$ and MnO_x and milled by MA method in a stainless steel (SS) jar using a planetary ball mill (RETSCH PM 200) with SS balls (10 mm dia.) for 6 hrs. The mixtures were then pressed into pellet and heated at 700^{o}C, 800^{o}C and 900^{o}C in oxygen for 4 hrs.

Morphology of the spinel $LiMn_2O_4$was studied by Scanning Electron Microscope (SEM) method at Center for Science and Technology of Advanced Materials (PSTBM), Puspiptek Serpong, Indonesia. Phase analyses were conducted by XRD method using Rigaku SmartLab XRD at KEK Tokai Campus, Japan. Crystal structure of the spinel samples at room temperature were studied by neutron diffraction on iMATERIA (BL-20), at Materials and Life Science Facility (MLF), Japan-Proton Accelerator Research Complex (J-PARC), Tokai, Japan. The structural parameters were refined with Z-Rietveld [32, 33]. Electrochemical study of the spinel as cathode material in Li-ion battery was performed at Kanno and Hirayama's Lab. of Tokyo Institute of Technology, Yokohama, Japan. Electrochemical testing was performed in 2032 coin type cells with lithium foil as negative electrode. The electrolyte used was 1 M $LiPF_6$ in EC:DEC (3:7v/v). The assembled cells were charged and discharged within a voltage range of 2.0 – 4.8 V at a constant current density of 10 mA g^{-1}.

3. Results and Discussion

3.1. *Morphology by SEM*

Figure 1.a and 1.b-d showed morphology of the spinel-type $LiMn_2O_4$ synthesized by MA for 6 hrs before and after annealed at temperature range of 700 - 900°C in oxygen, respectively. Before annealing, agglomerated particles of the mixture are observed. After annealing at 700°C (figure 1.b) the morphology shows agglomerates with roughness on the surface, while the spinel annealed at 800°C (figure 1.c) shows agglomeration contains more distinct particulates on its surface with an average particle size of about 250 nm and narrow particle size distribution. The crystalized shape was clearly observed at 900°C with an average size of about 550 nm as shown in figure 1.d.

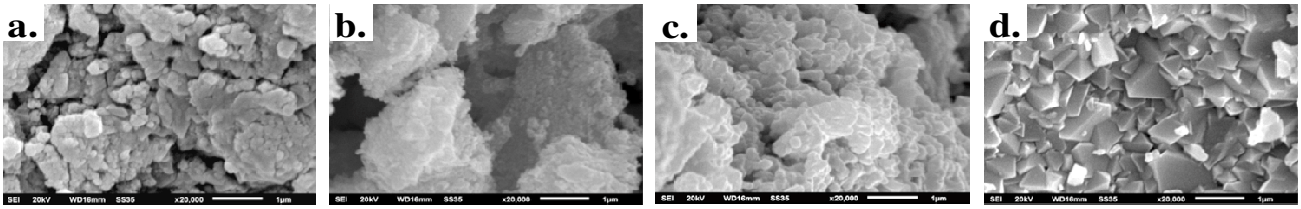

Figure 1. SEM micrograph of the spinel-type $LiMn_2O_4$ synthesized with an initial molar ratio of Li/Mn = 0.50 after MA for 6 hrs (a) before, and after annealing at (b) 700°C, (c) 800°C, and (d) 900°C for 4 hrs in oxygen.

3.2. *Phase and Crystal Structure by XRD*

Figure 2 shows XRD pattern for spinel $LiMn_2O_4$ after annealed at 700°C, 800°C and 900°C. The formation of spinel-type $LiMn_2O_4$ is shown for all annealed samples. However, the impurity from Mn_2O_3 and Li_2MnO_3 still appeared at 700°C. The crystal structure of the spinel $LiMn_2O_4$ belongs to space group *Fd-3m*. It is shown that the Bragg's peaks are getting sharper and higher with increasing temperature due to increasing crystallinity.

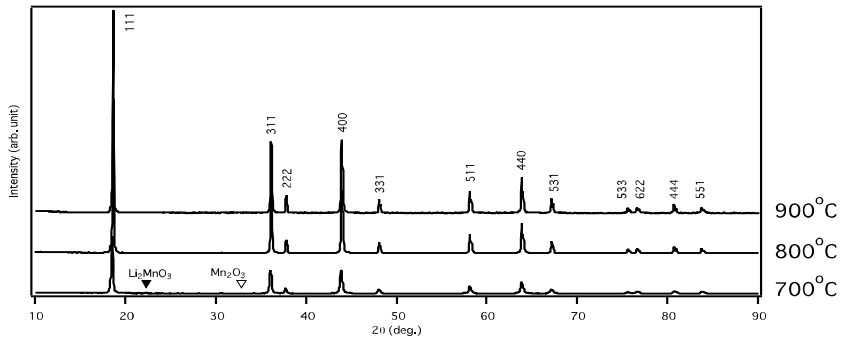

Figure 2. XRD patterns of the spinel-type $LiMn_2O_4$ synthesized with an initial molar ratio of Li/Mn = 0.50 by MA methods for 6 hrs and annealed at 700°C, 800°C and 900°C for 4 hrs in O_2.

3.3. *Crystal Structure by NPD*

In order to obtain detailed information on crystal structure and structural parameters, NPD is indispensable. Figure 3.a-c showed the Rietveld refinement patterns of neutron diffraction data of the spinel samples for various annealing temperatures with the interplanar spacings between 0.5 and 2.6 Å. All the patterns could be indexed using cubic spinel cell with space group *Fd-3m* and is consistent with the results of XRD.

The structural parameters were refined by adopting space group *Fd-3m* origin choice 2 using the model [12]: Li at 8*a* sites (1/8, 1/8, 1/8), Mn at 16*d* sites (1/2, 1/2, 1/2), and O at 32*e* sites (*x*, *x*, *x*) with $x \approx 0.26$. The refinement of the powder refinement data showing Fe and Cr that came from stainless steel jar and balls. Both atoms are positioned in Mn 16*d* sites with occupancies based on the chemical analysis using ICP-AAS [34]. The refinements result of neutron diffraction data at 700°C, 800°C and 900°C are listed in Tables 1, 2 and 3, respectively. The tables list the lattice constant and structural parameters with their estimated standard deviations in parentheses, and final *R* factors. The occupancy of Fe and Cr were fixed during the refinement of the neutron diffraction data for all $LiMn_2O_4$ samples, while the occupancy for Li, Mn, and O were varied. As the result, the occupancy of oxygen was found to be smaller than 1. The effect of annealing temperature to the content of oxygen is shown, where the occupancy of oxygen decreases with increasing annealing temperature. The occupancy of oxygen for the sample annealed at 700°C decreased to 0.9737 as shown in table 1. As the annealing temperature increased to 800°C, more oxygen was lost and the occupancy decreased further to 0.9705 as shown in table 2. Table 3 shows that the lost of oxygen is progressively increased and the occupancy of the oxygen for the sample annealed at 900°C is 0.9700.

The annealing temperature dependence of lattice constant, oxygen occupancy, manganese valence and lithium occupancy of the spinel samples are shown in figures 4.a-d. During refinement, vacancies were found in the oxygen 32*e* site and changed systematically with temperature and thus affected manganese valence in $LiMn_2O_4$ compound. Naturally, the existence of Fe in Mn 16*d* site will increase the Mn valence. The effect of oxygen lost, however, gives more impact and thus, resulted in decreasing of Mn valence. Therefore, it is clear that the oxygen occupancy decreased with increasing annealing temperatures. So that, the manganese valence decreased, while the lattice constant increased. It is related to Mn radius, whereas the radius of Mn^{3+} ion (0.0645 nm) is higher than Mn^{4+} (0.0530 nm). It is also found that lithium occupancy increases with increasing annealing temperature. Figure 4.e. showed the temperature

dependence of Li–O and Mn–O distances of the spinel samples, where both distances increased with temperature. Those can be related to the decreasing of oxygen occupancy and the average manganese valence as shown in figures 4.b-c. The Mn–O distances is related to Mn radius as previously explained. Figure 4.b and 4.e. show the relationship between oxygen occupancy and Li–O distances, where Li–O distances increases with decreasing oxygen occupancy.

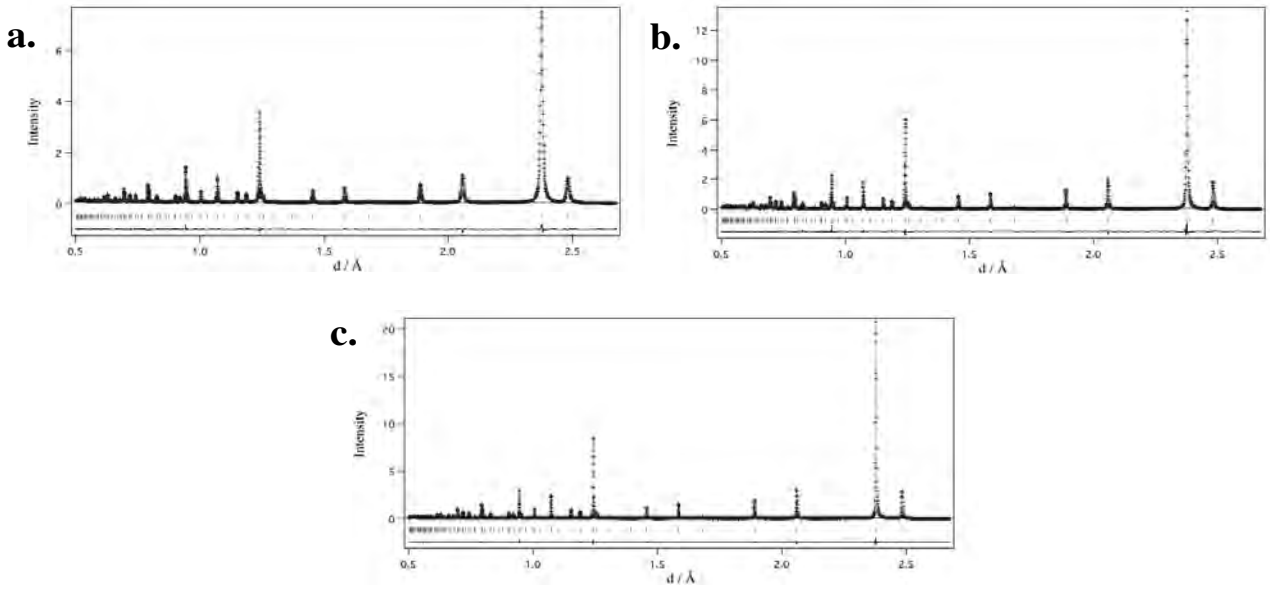

Figure 3. Rietveld refinement patterns of neutron diffraction data for spinel $LiMn_2O_4$ annealed at (a) 700°C, (b) 800°C, and (c) 900°C in O_2 from starting materials $LiOH.H_2O$ and MnO_x and a Li/Mn ratio of 1/2.

Table 1. Rietveld refinement results of spinel $LiMn_2O_4$ annealed at 700°C in O_2.

Atom	site	*g*	*x*	*y*	*z*	*B*/Å^2
Li(1)	8*a*	0.9536(41)	1/8	1/8	1/8	1.000(17)
Mn(1)	16*d*	0.9660	1/2	1/2	1/2	0.718(5)
O(1)	32*e*	0.9737(14)	0.26296(1)	= *x*(O1)	= *x*(O1)	1.153(5)
Fe	16*d*	0.0105	1/2	1/2	1/2	= *B*(Mn1)
Cr	16*d*	0.0017	1/2	1/2	1/2	= *B*(Mn1)
Atom	B_{11}/Å^2	B_{22}/Å^2	B_{33}/Å^2	B_{12}/Å^2	B_{13}/Å^2	B_{23}/Å^2
Li(1)	1.034(27)	= B_{11}(Li1)	= B_{11}(Li1)	0	0	0
Mn(1)	0.727(7)	= B_{11}(Mn1)	= B_{11}(Mn1)	-0.154(6)	= B_{12}(Mn1)	= B_{12}(Mn1)
O(1)	1.158(5)	= B_{11}(O1)	= B_{11}(O1)	-0.283(3)	= B_{12}(O1)	= B_{12}(O1)

Space group *Fd-3m*, a = 8.233316(8) Å, R_{wp} = 4.54, R_p = 3.78, R_e = 2.68, $S = R_{wp}/R_e$ = 1.69, R_B = 1.43, R_F = 3.15

Table 2. Rietveld refinement results of spinel $LiMn_2O_4$ annealed at 800°C in O_2.

Atom	site	*g*	*x*	*y*	*z*	*B*/Å^2
Li(1)	8*a*	0.9723(42)	1/8	1/8	1/8	1.050(17)
Mn(1)	16*d*	0.9627	1/2	1/2	1/2	0.700(5)
O(1)	32*e*	0.9705(14)	0.26296(1)	= *x*(O1)	= *x*(O1)	1.198(5)
Fe	16*d*	0.0139	1/2	1/2	1/2	= *B*(Mn1)
Cr	16*d*	0.0024	1/2	1/2	1/2	= *B*(Mn1)
Atom	B_{11}/Å^2	B_{22}/Å^2	B_{33}/Å^2	B_{12}/Å^2	B_{13}/Å^2	B_{23}/Å^2
Li(1)	1.090(27)	= B_{11}(Li1)	= B_{11}(Li1)	0	0	0
Mn(1)	0.711(7)	= B_{11}(Mn1)	= B_{11}(Mn1)	-0.162(5)	= B_{12}(Mn1)	= B_{12}(Mn1)
O(1)	1.198(5)	= B_{11}(O1)	= B_{11}(O1)	-0.277(3)	= B_{12}(O1)	= B_{12}(O1)

Space group *Fd-3m*, a = 8.239790(5) Å, R_{wp} = 4.74, R_p = 4.05, R_e = 3.10, $S = R_{wp}/R_e$ = 1.53, R_B = 1.32, R_F = 3.55

Table 3. Rietveld refinement results of spinel $LiMn_2O_4$ annealed at 900°C in O_2.

Atom	site	*g*	*x*	*y*	*z*	*B*/Å^2
Li(1)	8*a*	0.9845(40)	1/8	1/8	1/8	1.104(15)
Mn(1)	16*d*	0.9676	1/2	1/2	1/2	0.681(4)
O(1)	32*e*	0.9700(13)	0.26296(1)	= *x*(O1)	= *x*(O1)	1.195(4)
Fe	16*d*	0.0107	1/2	1/2	1/2	= *B*(Mn1)
Cr	16*d*	0.0017	1/2	1/2	1/2	= *B*(Mn1)
Atom	B_{11}/Å^2	B_{22}/Å^2	B_{33}/Å^2	B_{12}/Å^2	B_{13}/Å^2	B_{23}/Å^2
Li(1)	1.147(25)	= B_{11}(Li1)	= B_{11}(Li1)	0	0	0
Mn(1)	0.698(7)	= B_{11}(Mn1)	= B_{11}(Mn1)	-0.169(5)	= B_{12}(Mn1)	= B_{12}(Mn1)
O(1)	1.195(5)	= B_{11}(O1)	= B_{11}(O1)	-0.283(3)	= B_{12}(O1)	= B_{12}(O1)

Space group *Fd-3m*, a = 8.244564(4) Å, R_{wp} = 4.99, R_p = 4.21, R_e = 3.11, $S = R_{wp}/R_e$ = 1.60, R_B = 1.41, R_F = 4.06

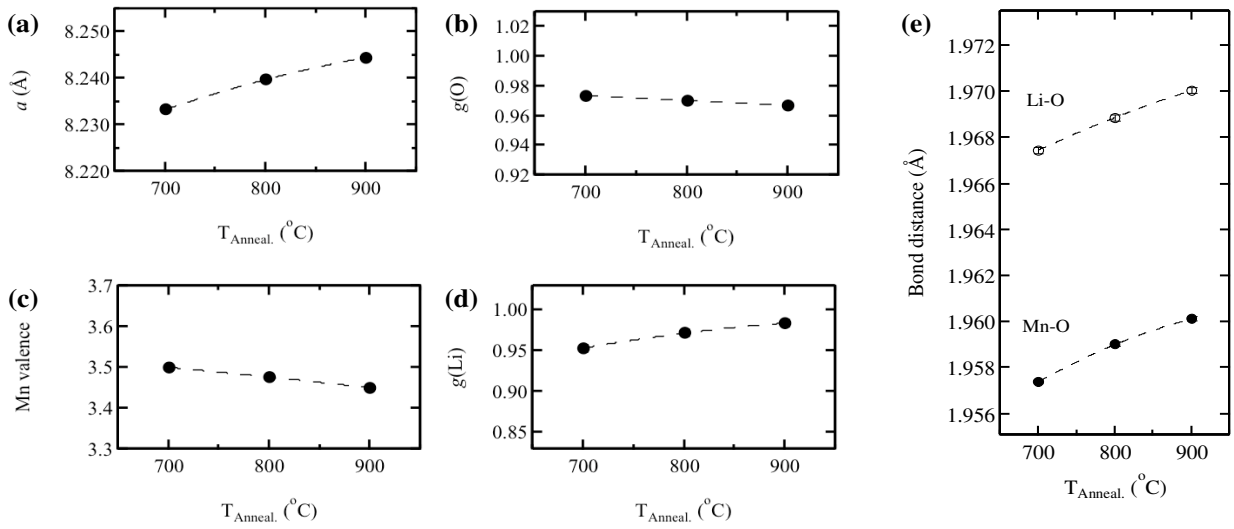

Figure 4. (a) Lattice constant, (b) oxygen occupancy, (c) manganese valence, (d) lithium occupancy, and (e) bond distances (Li–O, Mn–O) as a function of annealing temperature of the spinel-type $LiMn_2O_4$.

3.4. *Electrochemical Performance of the Spinel $LiMn_2O_4$*

The variation of first charge-discharge curves after cycled at 10 mA g^{-1} over the potential range of 2.0 – 4.8 V of the spinel $LiMn_2O_4$ synthesized by MA for 6 hrs and annealed in O_2 for 4 hrs at 700°C, 800°C and 900°C are shown in figure 5.

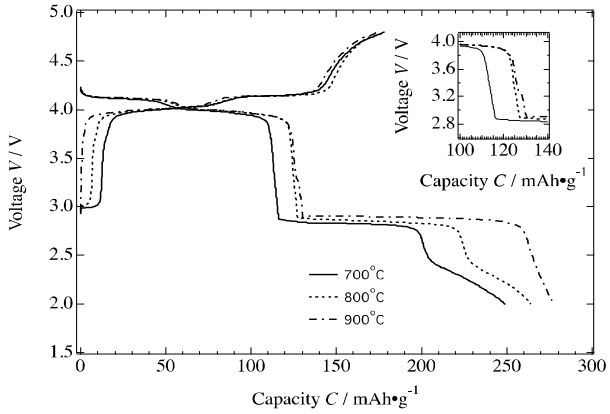

Figure 5. A continuous discharge curves over the potential range of 2.0 – 4.8 V at a constant current density of 10 mA g^{-1} for the Li/1M $LiPF_6$ – EC/DEC solution/porous $LiMn_2O_4$ cells using spinels $LiMn_2O_4$ powder annealed at 700–900°C in O_2.

The discharge capacities and voltage plateaus are increased with increasing temperature. The initial discharge capacity increases from 248.95 mAh g^{-1} to 264.29 mAh g^{-1} and finally to 277.24 mAh g^{-1} and the three voltage plateaus were shifted to higher voltages as the annealing temperature increases from 700°C to 800°C and to 900°C, respectively. In addition, the length of plateau increases with temperature. It is related to the crystallinity of the material and increasing lattice constant *a* with temperature. The lower crystallization of the sample annealed at lower temperature, i.e. 700°C, caused a small coulombic repulsive reaction [35]. In the material with low crystallinity, a number of cation defect is formed which results in disproportion occupancy of tetrahedral and octahedral cation. Therefore, the material annealed at lower temperature has lower discharge potential [36]. The initial discharge capacity increased at 800°C due to higher crystallinity and purity. The initial discharge capacity then increased further for the material annealed at 900°C. However, it is worth noting that a pseudo plateau was occurred at voltage around 3.27 V as shown in the inset of figure 5 related to further intercalation of Li in the stoichiometric $LiMn_2O_4$ spinel and lead to the transformation from cubic $Li[Mn_2]O_4$ to tetragonal $Li_2[Mn_2]O_4$.

4. Conclusion

Spinel $LiMn_2O_4$ powder for cathode material in Li-ion battery have been synthesized by MA method and subsequent annealing at different temperatures. It is found that the initial discharge capacity of the Li-ion battery increased with annealing temperature and reached the highest at 277.24 mAh g^{-1} after annealed at 900^{o}C. It is related to the increasing crystallinity and purity of the spinel $LiMn_2O_4$ as shown by the results from SEM and XRD. The results from NPD showed that lattice constant increased with temperature, related to the increasing crystallinity. Characterization and analyses of the obtained spinel samples showed relationship between annealing temperature and characteristic of the spinel such as crystallinity, composition, structural parameters and electrochemical behavior.

Acknowledgement

T.Y.S.P.P. is grateful for all support kindly provided by MEXT Japan. Valuable discussion and suggestion from the members of Powder Diffraction Group in KEK and J-PARC, from the members of Kanno and Hirayama's Lab., and from Prof. T. Sakuma of Ibaraki University are greatly acknowledged.

References

1. A. Yamada and M. Tanaka, *Mat. Res. Bull.* **30(6)**, 715 (1995).
2. W. T. Jeong, J. H. Joo and K. S. Lee, *J. Alloys and Compounds* **358**, 294 (2003).
3. W. T. Jeong, J. H. Joo and K. S. Lee, *J. Power Sources* **119–121**, 690 (2003).
4. S. H. Ye, J. Y. Lv, X. P. Gao, F. Wu and D. Y. Song, *ElectrochimicaActa* **49**, 1623 (2004).
5. L. J. Ning, Y. P. Wu, S. B. Fang, E. Rahm and R. Holze, *J. Power Sources* **133**, 229 (2004).
6. J-M. Tarascon, M. Morcrette, J. Saint, L. Aymard and R. Janot, *C. R. Chimie* **8**, 17 (2005).
7. A. Yamada, *J. Solid State Chem.* **122**, 160 (1996).
8. A. Yamada, M. Tanaka, K. Tanaka and K. Sekai, *J. Power Sources* **81-82**, 73 (1999).
9. N. V. Kosova, I. P. Asanov, E. T. Devyatkina and E. G. Avvakumov, *J. Solid State Chem.* **146**, 184 (1999).
10. N. V. Kosova, N. F. Uvarov, E. T. Devyatkina and E. G. Avvakumov, *Solid State Ionics* **135**, 107 (2000).
11. N. V. Kosova, E. T. Devyatkina and S. G. Kozlova, *J. Power Sources*, **97-98**, 406 (2001).

12. M. Yonemura, *Synthesis, Crystal Structure, and Physical Properties of Lithium Containing Cathode Materials with the Spinel and Olivine Structure*, Doctoral Thesis, Kobe: Kobe University, (2004).
13. Y. -K. Sun, *Solid State Ionics* **100**, 115 (1997).
14. Y. -K. Sun, I. -H. Oh and K. Y. Kim, *Ind. Eng. Chem. Res.* **36**, 4839 (1997).
15. Y. -K. Sun and I. -H. Oh, *J. Power Sources* **94**, 132 (2001).
16. Y. -K. Sun, S. W. Oh, C. S. Yoon, H. J. Bang, and J. Prakash, *J. Power Sources* **161**, 19 (2006).
17. L. Tao, Q. Weihua, Z. Hailei and L. Jingjing, *Materials Letters* **60**, 1251 (2006).
18. A. S. Wills, N. P. Raju and J. E. Greedan, *Chem. Mater.* **11**, 1510 (1999).
19. X. Q. Yang, X. Sun, M. Balasubramanian, J. McBreen, Y. Xia, T. Sakai and M. Yoshio, *Electrochemical and Solid-State Letters* **4 (8)**, A117-A120 (2001).
20. J-M. Tarascon and D. Guyomard, *Electrochimica Acta* **38: 9**, 1221 (1993).
21. D. Guyomard and J-M. Tarascon, *Solid State Ionics* **69**, 222 (1994).
22. P. Barboux, J-M. Tarascon and F. K. Shokoohi, *J. Solid State Chem.* **94**, 185 (1991).
23. S-W. Jang, H-Y. Lee, K-C. Shin, S.M. Lee, J-K. Lee, S-J. Lee, H-K. Baik and D-S. Rhee, *J. Power Sources* **88**, 274 (2000).
24. X. He, L. Wang, W. Pu, G. Zhang, C. Jiang and C. Wan, *Int. J. Electrochem. Sci.* **1**, 12 (2006).
25. A. Lagashetty, V. Havanoor, S. Basavaraja and A. Venkataraman, *Indian Journal of Chemical Technology* **15**, 41 (2008).
26. M. Helan, L. J. Berchmans, and A. Z. Hussain, *Ionics* **16**, 227 (2010).
27. Y. Xia, H. Takeshige, H. Noguchi and M. Yoshio, *J. Power Sources* **56**, 61 (1995).
28. Y-S. Lee, N. Kumada and M. Yoshio, *J. Power Sources* **96**, 376 (2001).
29. Y-S. Lee, S-J. Cho and M. Yoshio, *Korean J. Chem. Eng.* **23(4)**, 566 (2006).
30. Y. Wei, K. B. Kim, G. Chen and C. W. Park, *Materials Characterization* **59**, 1196 (2008).
31. X. Jin, Z. Hua-li, C. Zhao-yong, P. Zhong-dong and H. Guo-rong, *Trans. Nonferrous Met. Soc. China* **16**, 467 (2006).
32. R. Oishi .et al., *Nuclear Instruments and Methods in Physics Research* A **600**, 94–96 (2009).
33. High Energy Accelerator Research Organization, *User's guide for Z-Rietveld.* Tsukuba: KEK. (2009).
34. Unpublished data.
35. Y. M. Hon, H. Y. Chung, K. Z. Fung and M. H. Hon *J. Solid State Chem.* **160**, 368 (2001).
36. T. F. Yi, C-L. Hao, C-B. Yue, R-S. Zhu and J. Shu, *Synthetic Metals* **159**, 1255 (2009).